



---

*Research article*

## **A study on the transmission and dynamical behavior of an HIV/AIDS epidemic model with a cure rate**

**Attaullah<sup>1,\*</sup>, Sultan Alyobi<sup>2</sup> and Mansour F. Yassen<sup>3,4</sup>**

<sup>1</sup> Department of Mathematics & Statistics, Bacha Khan University Charsadda 24461, Pakistan

<sup>2</sup> King Abdulaziz University, College of Science & Arts, Department of Mathematics, Rabigh, Saudi Arabia

<sup>3</sup> Department of Mathematics, College of Science and Humanities in Al-Aflaj, Prince Sattam Bin Abdulaziz University, Al-Aflaj 11912, Saudi Arabia

<sup>4</sup> Department of Mathematics, Faculty of Science, Damietta University, New Damietta 34517 Damietta, Egypt

\* **Correspondence:** Email: [attaullah@bkuc.edu.pk](mailto:attaullah@bkuc.edu.pk).

**Abstract:** In developing nations, the human immunodeficiency virus (HIV) infection, which can lead to acquired immunodeficiency syndrome (AIDS), has become a serious infectious disease. It destroys millions of people and costs incredible amounts of money to treat and control epidemics. In this research, we implemented a Legendre wavelet collocation scheme for the model of HIV infection and compared the new findings to previous findings in the literature. The findings demonstrate the precision and practicality of the suggested approach for approximating the solutions of HIV model. Additionally, establish an autonomous non-linear model for the transmission dynamics of healthy  $CD4^+$  T-cells, infected  $CD4^+$  T-cells and free particles HIV with a cure rate. Through increased human immunity, the cure rate contributes to a reduction in infected cells and viruses. Using the Routh-Hurwitz criterion, we determine the basic reproductive number and assess the stability of the disease-free equilibrium and unique endemic equilibrium of the model. Furthermore, numerical simulations of the novel model are presented using the suggested approach to demonstrate the efficiency of the key findings.

**Keywords:** HIV/AIDS; LWCM-method; Numerical comparison

**Mathematics Subject Classification:** 34A12, 34K28

---

## 1. Introduction

Human immunodeficiency virus (HIV) infection is a serious health risk for many people across the world. It is a virus that spreads via bodily fluids and affects the human immune system, specifically  $CD4^+$  T cells, commonly known as T cells. Furthermore, it is anticipated that it would do so much harm to these cells that the human body will be unable to fight diseases and illnesses. As an illness and a cause of prejudice, HIV/AIDS has a profound impact on society. Acquired Immunodeficiency Syndrome (AIDS) is an incredibly dangerous infectious disease that has roused the interest of researchers all over the world. HIV is the causative agent, which undermines the immunological function of  $CD4^+$  T-cells in the human body in order to get its uncontrolled proliferation. According to a report from the World Health Organization (WHO), there are 37.7 million people affected. Mathematical models for the transmission of HIV/AIDS often incorporate progressive growth in which an individual infected with HIV may progress through several infectious stages [1,2]. Once an individual has carried a level of infectious disease, there is no way to hold back [3]. This presumption had to be changed when highly active antiretroviral treatment (HARRT) was introduced in 1996. The cure extends the time available for HIV/AIDS transmission [3]. Individuals who are taking medical treatment have a lower risk of spreading the disease to others. Therefore, one should focus on educating infected patients who are continuously seeking treatment in order to help the administration to control the transmission of HIV/AIDS [4]. Mathematical analysis has been shown to be an effective tool for better understanding disease dynamics, predicting communicable diseases, and evaluating protection or assistance strategies [5]. Hence, in recent decades, numerous researchers have developed a wide range of mathematical models to study the dynamical characteristics of HIV/AIDS (see [6–12] for details information). HIV expression has been shown to be a chaotic system that results in a considerable variability in retroviral production [13]. Mao et al. [14] observed that a small amount of environmental variation in the model prevents a significant increase in population. To demonstrate this inherently fascinating fact, they stochastically perturb the multivariate deterministic system and illustrate that the original ordinary differential equation may explode to infinity in a limited time, with probability one that of the associated stochastic differential equation does not. Ogunlaran et al. [15] presented a mathematical model comprising two control parameters in which uninfected  $CD4^+$  T cells proliferate in a logistic manner and the incidence term is saturated with free viral particles. They utilized the efficacy of pharmacological therapy to prevent the infection of cells and the formation of new free viral particles. Duffin et al. [16] investigated the dynamics of the immunodeficiency virus during the course of the infection cycle. They suggested two comprehensive models that properly anticipate the dynamics of the infection by considering variables for chronic loss of  $CD4^+$  T cells and variations in viral clearance and generation. They concluded that both the viral clearing model and the macrophage reservoir model could identify the anticipated decrease in the number of T cells and increase in the number of viruses that occur when AIDS is first diagnosed. Omondi et al. [17] studied the modelling of the influence of HIV transmission, therapeutic interventions, and regulation in Kenya. They concluded that both the viral clearance model and the macrophage reservoir model could predict the expected drop in the population of T cells and the rise in the number of viruses that happen when AIDS starts. For HIV modeling, Wodarz et al. [18] established the etiology and therapeutic compartments for HIV modeling. They presented a foundational model of viral infection and described how it would be used to investigate HIV movements and quantify crucial parameters, resulting in a better understanding of the disease process. They introduced the idea of variety threshold as an

illustration of how viral evolution may contribute to disease progression and immune system dysfunction. They demonstrated that how mathematical models may be used to comprehend the characteristics of long-term immunological control of HIV and to develop therapy regimens that can transform a progressing individual to a stage of protracted non-progression. Ida et al. [19] evaluated the deterministic model of HIV infection using a nonlinear dynamical analysis. In Cuba, Mastroberardino et al. [20] explored the virus's dynamics. The highly successful national preventive programme of Cuba considered the mechanism of transmission via contact with undiagnosed HIV-positive individuals. They determined the equilibria of the governing nonlinear system, performed a linear stability analysis, and then provided results based on global stability. Attaullah et al. [21] implemented a numerical technique for finding the dynamics of infectious illnesses in humans and presented the effect of different non-linear supply rate on the dynamics of HIV infection model. Theys et al. [22] investigated the effect of HIV-I transmission patterns on host evolution. Bozkurt et al. [23] studied the stability analysis of the HIV epidemic model. Nosova et al. [24] designed a model to study the effects of the transmission of HIV and interactions in the human population. They examined the model and discussed that how the HIV spreads, which includes the virus and how risk groups change over time. Theys et al. [22] investigated the impacts of HIV-I infection variations on host adaptation. Bozkurt et al. [23] analyzed the stability of the HIV epidemic model. Nosova et al. [24] developed a framework to investigate the consequences of disease transmission and human population interactions. They explored the transmission model of HIV that included the dynamics of the vulnerability group. Sun et al. [25] examined the assessment of HIV incidence rates using various mathematical models. By adding the optimal control technique to the fractional order derivative, Sweilam et al. [26] investigated HIV/AIDS and malaria illness modelling. Ongun [27] implemented the Laplace Adomian decomposition method (LADM) to approximate the HIV infection solution and discussed the reliability and simplicity of the methods. Merdan [28] performed the variational iteration method (VIM), modified VIM to provide an approximation of the HIV model, and displayed the results to demonstrate the consistency and effectiveness of the techniques. Yüzbaşı [29] used the Bessel collocation method (BCL) to approximate the HIV infection solution. Doğan [30] used the multistep Laplace Adomian decomposition method (MLADM) to find the numerical solution of the HIV model. Gandomani [31] applied the Müntz-Legendre Polynomials technique to solve the HIV model numerically. Parand et al. [32] employed the Quasi-linearization Lagrangian method (QLM) for finding the numerical solution of the HIV model. Attaullah et al. [33] employed the Galerkin time discretization approach for the HIV disease transmission dynamics with a non-linear supply rate. Iqbal et al. [34] addressed the positivity and boundedness preservation method for the solution of the fractional nonlinear HIV/AIDS epidemic model. Günerhan et al. [35] examined the HIV fractional model employing Caputo and constant proportional Caputo operators. Gaomet al. [36] explored the analytical and approximate solutions of an HIV/AIDS pandemic system. The aforementioned computational analysis has captivated our interest in developing a novel approach to the HIV model. The main objective of the research is to use a Legendre wavelet collocation scheme for approximating the HIV model. Our second goal is to compare the solutions of the suggested methodology to the findings of the well-known fourth order Runge-Kutta method (RK4-method) and other techniques exists in the literature. The third objective of the study is to introduce a new model by including treatment rate and analysis of the developed model based on the basic reproduction number and stability of the new model. Several individuals with symptomatic characteristics may be transitioned into asymptomatic individuals via various therapy strategies. One of the major goals is to investigate

how the therapy affects the disease's protracted behavior. The findings indicate that depending on the parameter values, therapy may result in the illness persisting or fading out. The other is to examine the influence of the cure rate on the stability of the endemically diseased equilibrium. Further, we assessed how the cure rate affects the concentration of healthy T-cells, infected T-cells, and free viruses. Medically speaking, this indicates that the model with cure rate decreases infected cells and viruses by enhancing human immunity. In addition, equip clinicians with adequate information to minimize the viral load of the infection. Noteworthy real-world problems may be handled utilizing the suggested methodology. All the computations are carried out using the Mathematica software for Legendre wavelet collocation scheme and the MATLAB software for the Runge-Kutta technique.

The remainder of the article is organized as follows: Section 2 introduces the fundamental formulation of the HIV model. Sections 3 and 4 provide the well-known Legendre wavelet collocation and Runge-Kutta method implemented for the model. Numerical results and comparison analysis for the solutions of the suggested scheme with other classical techniques applied to the model are discussed in Section 5. The innovative model's analysis is presented in Section 6. Section 7 gives the conclusions and future recommendations of the article.

## 2. Basic mathematical formulation of HIV model

The mathematical modeling of disease or natural phenomena is a major field of study for mathematicians and biologists. According to the mathematical model, transmissible disorders may be illustrated in partial/ordinary differential equations (PDEs)/(ODEs), or both. It is essential to examine the dynamical behavior, reproduction number, stability analysis, bifurcation analysis, and computational findings of models that represent the epidemiology of a certain disorder. Several mathematical models for different contagious diseases have been presented since the inception of this model. HIV is a virus that attacks healthy T-cells, which is a kind of white blood cell. Numerous mathematical models of this crippling disease have been extensively researched. The primary purpose of such mathematical models is to get insights into disease mechanisms and how to mitigate the disease. Herein, we considered a mathematical model proposed by Parand et al. [32] consists of three first-order nonlinear differential equations that characterize the dynamics of healthy/infected T-cells and free virus particles. The population of healthy T-cells represented by  $T(t)$ , infected T-cells by  $I(t)$ , and virus particles by  $V(t)$  which is described as follow:

$$\frac{dT}{dt} = \gamma - \omega T + \rho T \left(1 - \frac{T+I}{T_{max}}\right) - \chi VT, \quad (2.1)$$

$$\frac{dI}{dt} = \chi VT - \delta I, \quad (2.2)$$

$$\frac{dV}{dt} = N\delta I - dV, \quad (2.3)$$

Table 1 summarizes the initial conditions of the state variables and a detailed description of each parameter involved in the model.

**Table 1.** The description of parameters and their corresponding values involved in the model. The unit for the parameters is days<sup>-1</sup>mm<sup>-3</sup>.

Parameters	Explanations	Values [32,35]
$T(0)$	Density of healthy T-cells	0.1
$I(0)$	Density of infected T-cells	0.0
$V(0)$	Density of virus	0.1
$\gamma$	Production of healthy T-cells	0.1
$\omega$	Natural death rate of healthy T-cells	3.0
$\delta$	Natural death rate of infected T-cells	0.3
$\rho$	Growth rate of T-cells	3.0
$d$	The virus death rate	2.4
$\chi$	The incidence with which T-cells get infected with a viral	0.0027
$N$	Density of virus particles generated by infected T-cells	10
$T_{max}$	Maximum density of healthy T-cells	1500
$p$	Rate of cure	0.01

### 3. Description of LWCM for HIV infection model

The wavelet has an enormous range of applications in technology and research. The use of wavelets in approximation theory has increased in popularity over the last decades. This section incorporates the LWCM for the HIV model, which is based on Legendre polynomials. The Legendre wavelet is used to approximate the unknown function. To get the system of algebraic equations, the collocation points are investigated. The Legendre wavelet's orthogonality enables the calculation of coefficients of expansion. Another significant advantage of using the wavelets approach is the sparsity of the coefficient matrix of the final system of equations. In innovation and science, the wavelet has a wide range of applications. Wavelets have grown in prominence in approximation theory during the past several decades. The Legendre wavelet collocation method (LWCM) has been successfully implemented to solve ordinary differential equations, partial differential equations, and fractional differential equations (see [37–40] for details). The LWCM is a powerful tool for statistically analyzing real-world problems. Dizicheh et al. [41] used the Legendre wavelet spectral collocation approach to tackle oscillatory initial value problems. Kajani et al. [42] solved the linear integro-differential equation using the Legendre wavelets method. Abbaszadeh et al. [43] solved fractional Fredholm integro-differential equations using the Legendre wavelets method.

#### 3.1. Legendre wavelet

The Legendre wavelet [44] is defined on  $[0,1]$  and is given by

$$\psi_{n,m}(t) = \begin{cases} \sqrt{m + \frac{1}{2}} \frac{k}{2^k} P_m(2^k t - 2n + 1), & \frac{n-1}{2^{k-1}} \leq t \leq \frac{n}{2^{k-1}}, \\ 0, & \text{otherwise} \end{cases} \quad (3.1)$$

where  $n = 1, 2, 3, \dots, 2^{k-1}$ ,  $m = 0, 1, 2, 3, \dots, M - 1$ ,  $k, M$  are positive integers, and the coefficient  $\sqrt{m + \frac{1}{2}}$  is for orthonormality, and  $k, M$  are positive integers. On the interval  $[-1,1]$ , the Legendre

polynomials of order  $m$  are defined and are given by the recurrence relations  $P_m(t)$ .

$$P_0(t) = 1,$$

$$P_1(t) = t,$$

$$P_{m+1}(t) = \left(\frac{2m+1}{m+1}\right) tP_m(t) - \left(\frac{m}{m+1}\right) P_{m-1}(t). \quad m = 1, 2, 3 \dots$$

We can approximate a function as a linear combination of Legendre wavelets because they provide an orthonormal basis for  $L^2(\mathbb{R})$ .

### 3.2. Implementation of LWCM to HIV model

In this section, we employed the LWCM to the models described by system of non-linear differential equations (2.1)–(2.3) and Eqs (6.1)–(6.3). According to LWCM.

$$T(t) = \sum_{n=1}^{2^{k-1}} \sum_{m=0}^{M-1} q_{n,m} \psi_{n,m}(t) = Q\psi(t), \quad (3.2)$$

$$I(t) = \sum_{n=1}^{2^{k-1}} \sum_{m=0}^{M-1} r_{n,m} \psi_{n,m}(t) = R\psi(t), \quad (3.3)$$

$$V(t) = \sum_{n=1}^{2^{k-1}} \sum_{m=0}^{M-1} s_{n,m} \psi_{n,m}(t) = S\psi(t). \quad (3.4)$$

The nonlinear terms are approximated as:

$$T^2(t) = \sum_{n=1}^{2^{k-1}} \sum_{m=0}^{M-1} k_{n,m} \psi_{n,m}(t) = K\psi(t), \quad (3.5)$$

$$T(t)I(t) = \sum_{n=1}^{2^{k-1}} \sum_{m=0}^{M-1} x_{n,m} \psi_{n,m}(t) = X\psi(t) \quad (3.6)$$

$$V(t)I(t) = \sum_{n=1}^{2^{k-1}} \sum_{m=0}^{M-1} g_{n,m} \psi_{n,m}(t) = G\psi(t), \quad (3.7)$$

where  $Q, R, S, K, X, G$ , and  $\psi$  are  $2^{k-1} \times M$  matrices given by:

$$Q = [q_{1,0}, \dots, q_{1,M-1}, \dots, q_{2,M-2}, \dots, q_{2^{k-1},0}, \dots, q_{2^{k-1},M-1}],$$

$$R = [r_{1,0}, \dots, r_{1,M-1}, \dots, r_{2,M-2}, \dots, r_{2^{k-1},0}, \dots, r_{2^{k-1},M-1}],$$

$$S = [s_{1,0}, \dots, s_{1,M-1}, \dots, s_{2,M-2}, \dots, s_{2^{k-1},0}, \dots, s_{2^{k-1},M-1}]$$

$$K = [k_{1,0}, \dots, k_{1,M-1}, \dots, k_{2,M-2}, \dots, k_{2^{k-1},0}, \dots, k_{2^{k-1},M-1}],$$

$$X = [x_{1,0}, \dots, x_{1,M-1}, \dots, x_{2,M-2}, \dots, x_{2^{k-1},0}, \dots, x_{2^{k-1},M-1}],$$

$$G = [g_{1,0}, \dots, g_{1,M-1}, \dots, g_{2,M-2}, \dots, g_{2^{k-1},0}, \dots, g_{2^{k-1},M-1}],$$

$$\psi = [\psi_{1,0}, \dots, \psi_{1,M-1}, \dots, \psi_{2,M-2}, \dots, \psi_{2^{k-1},0}, \dots, \psi_{2^{k-1},M-1}].$$

Using Eqs (3.2)–(3.7) in Eqs (2.1)–(2.6) we get

$$Q^T \psi'(t) = \gamma - \omega Q^T \psi(t) + \rho Q^T \psi(t) - \frac{\rho}{T_{max}} (K^T \psi(t) + X^T \psi(t) - \chi G^T \psi(t)), \quad (3.8)$$

$$R^T \psi'(t) = \chi G^T \psi(t) - \delta R^T \psi(t), \quad (3.9)$$

$$S^T \psi'(t) = R \delta R^T \psi(t) - d S^T \psi(t), \quad (3.10)$$

$$Q^T \psi(0) = 0.1, \quad (3.11)$$

$$R^T \psi(0) = 0, \quad (3.12)$$

$$S^T \psi(0) = 0.1. \quad (3.13)$$

Now collocating equations (3.8)–(3.10) and Eqs (3.5)–(3.7) at

$$t_j = \frac{j-0.5}{2^{k-1}M}, \quad (3.14)$$

where  $(j = 1, 2, 3, \dots, 2^{k-1}M - 1)$  for Eqs (3.8)–(3.10) and  $(j = 1, 2, 3, \dots, 2^{k-1}M)$  for Eqs (3.5)–(3.7), we obtained the following equations:

$$Q^T \psi'(t_j) = \gamma - \omega Q^T \psi(t_j) + \rho Q^T \psi(t_j) - \frac{\rho}{T_{max}} (K^T \psi(t_j) + X^T \psi(t_j) - \chi G^T \psi(t_j)), \quad (3.15)$$

$$R^T \psi'(t_j) = \chi G^T \psi(t_j) - \delta R^T \psi(t_j), \quad (3.16)$$

$$S^T \psi'(t_j) = R \delta B^T \psi(t_j) - d S^T \psi(t_j), \quad (3.17)$$

$$T^2(t_j) = K^T \psi(t_j), \quad (3.18)$$

$$T(t_j)I(t_j) = X^T \psi(t_j), \quad (3.19)$$

$$V(t_j)T(t_j) = G^T \psi(t_j). \quad (3.20)$$

From Eqs (2.1)–(2.6),  $6(2^{k-1}M)$  total unknown constants. We need  $6(2^{k-1}M)$  equations to find these constants, of which  $6(2^{k-1}M) - 3$  equations come from Eqs (3.14)–(3.19) while the remaining three equations come from Eqs (3.11)–(3.13). By solving the system of equations, we can obtain the unknown constants that can be used in Eqs (3.2)–(3.4) to obtain the required result.

#### 4. The Runge-Kutta method of order four

The fourth order Runge-Kutta method briefly the RK4 approach is a well-known technique used to solve numerically the first order initial value problems. This approach is usually employed for complicated problems and is able to deal with nonlinear phenomena (See [33,45,46] for details information).

#### 5. Comparative analysis

This section provides the HIV model solution using LWCM and the RK4-method along with comparisons of the findings to those reported in the literature. We compared the numerical solutions and absolute errors of the suggested method to other classical techniques (LADM [27], VIM [28], MVIM [28], MLCM [30], QL method [32]) relative to RK4 scheme are displayed in Tables 2–10 for  $I(t)$ ,  $V(t)$  and  $T(t)$  respectively. After comparison, it is observed that the proposed schemes yield more

accurate outcomes than the other methods used for the model. To address additional concerns, Figure 1(a)–(c) show the graphical results of the LWCM and QL techniques in comparison to the RK4 method. The results obtained by LWCM are effective when compared to the RK4-method. Additionally, we present the mesh grid graphs in Figure 2 for the results of all the methods used for the mentioned above model. Figure 1(a)–(c) and Tables 2–10 clearly demonstrate that the new techniques provide reasonably good agreement with the RK4-method results when compared to other classical approaches used for the HIV infection model. This validate that the RK4 and LWCM frameworks are capable of determining the behavior of these variables in the region under investigation.

**Table 2.** Results of  $T(t)$  in comparison with RK4 scheme.

$t$	LWCM	QL method [32]	RK4	QLM-RK4	LWCM-RK4
0.0	0.10000000	0.10000000	0.00100000	0.0000E-7	0.0000E-7
0.2	0.20880798	0.20880808	0.20880756	5.2366E-7	4.2482E-7
0.4	0.40624018	0.40624054	0.40623864	1.8999E-6	1.5414E-7
0.6	0.76442292	0.76442389	0.76441873	5.1680E-6	4.1935E-7
0.8	1.41404449	1.41404685	1.41403436	1.2488E-5	1.0135E-7
1.0	2.59158953	2.59159485	2.59156659	2.8261E-5	2.2944E-7

**Table 3.** Result of  $I(t)$  in comparison with RK4 scheme.

$t$	LWCM	QL method [32]	RK4	QLM-RK4	LWCM-RK4
0.0	0.000000E-0	0.00000000E-0	0.000000E-0	0.0000E-00	0.0000E-00
0.4	0.131583E-4	0.13158340E-4	0.131582E-4	1.2320E-10	1.0067E-10
0.6	0.212237E-4	0.21223785E-4	0.212235E-4	2.1007E-10	1.7116E-10
0.8	0.301773E-4	0.30177420E-4	0.301771E-4	3.1673E-10	2.5739E-10
1.0	0.400377E-4	0.40037815E-4	0.400373E-4	4.4638E-10	3.6195E-10

**Table 4.** Result of  $V(t)$  in comparison with RK4 scheme.

$t$	LWCM	QL method [32]	RK4	QLM-RK4	LWCM-RK4
0.0	1.00000000E-1	100000000000E-1	1.000000000E-2	0.00000E-00	0.0000E-00
0.2	6.18798517E-2	6.18798432237E-2	6.187989993E-2	5.67597E-08	4.8200E-08
0.4	3.82948983E-2	3.82948877731E-2	3.829495805E-2	7.02324E-08	5.9646E-08
0.6	2.37045598E-2	2.37045500445E-2	2.370461520E-2	6.51562E-08	5.5342E-08
0.8	1.46803717E-2	1.46803636840E-2	1.468041739E-2	5.36950E-08	4.5617E-08
1.0	9.10085126E-3	9.10084499664E-3	9.100886468E-3	4.14301E-08	3.5211E-08

**Table 5.** Assessment of the findings of LWCM with those of other traditional techniques for  $T(t)$ .

$t$	LWCM	RK4	LADM [27]	VIM [28]	MLCM [30]	MVIM [28]
0.0	0.100000000	0.100000000	0.100000000	0.100000000	0.100000000	0.100000000
0.2	0.208806496	0.208800678	0.208807329	0.208807321	0.208808084	0.208808086
0.4	0.406234784	0.406213674	0.406135831	0.406134658	0.406240543	0.406240794
0.6	0.764408254	0.764350814	0.762476222	0.762453035	0.766442390	0.764428724
0.8	1.414009061	1.413870248	1.398082863	1.397880588	1.414046852	1.414094173
1.0	2.591509458	2.591195190	2.507874151	2.506746669	2.591559480	2.591921076

**Table 6.** Assessment of the findings of LWCM with those of other traditional techniques for  $I(t)$ .

$t$	LWCM	RK4	LADM [27]	VIM [28]	MLCM [30]	MVIM [28]
0.0	0.000000000E-0	0.000000000E-0	0.000000000E-0	0.000000000E-0	0.000000E-0	0.10000000E-00
0.2	6.032546494E-6	6.031878972E-6	6.60327069E-5	6.6032634E-5	6.603270E-05	6.60327016E-05
0.4	1.315797854E-5	1.315648606E-5	0.13158910E-4	0.1314878E-4	0.131583E-04	0.13158301E-04
0.6	2.122315973E-5	2.122067760E-5	0.21232981E-4	0.2101417E-4	0.212237E-04	0.21223310E-04
0.8	3.017646616E-5	3.017281029E-5	0.30242701E-4	0.2795130E-4	0.301774E-04	0.30174509E-04
1.0	4.003645811E-5	4.003141584E-5	0.40333218E-4	0.2431562E-4	0.400378E-04	0.40025404E-04

**Table 7.** Assessment of the findings of LWCM with those of other traditional techniques for  $V(t)$ .

$t$	LWCM	RK4	LADM [27]	VIM [28]	MLCM [30]	MVIM [28]
0.0	0.100000000	0.100000000	0.100000000	0.100000000	0.100000000	0.100000000
0.2	0.061879980	0.061880847	0.061879953	0.061879953	0.061879843	0.061879908
0.4	0.038295057	0.038296130	0.038308180	0.038308201	0.038294888	0.038295957
0.6	0.023704707	0.023705703	0.023919816	0.023920292	0.023704550	0.023710294
0.8	0.014680493	0.014681314	0.016212343	0.016217045	0.014680364	0.014700419
1.0	0.009100944	0.009101579	0.016055022	0.016084187	0.009100845	0.009157238

**Table 8.** Assessment of absolute errors for  $T(t)$  of the LWCM with other conventional methods relative to RK4-method.

$t$	0.1	0.2	0.4	0.6	0.8	1.0
LWCM	0.0	5.18760E-6	2.11093E-5	5.74299E-5	1.38812E-4	3.14268E-4
LADM [27]	0.0	6.65092E-6	7.78434E-5	1.87459E-3	1.57873E-2	8.33210E-2
VIM [28]	0.0	6.64252E-6	7.90162E-5	1.89777E-3	1.59896E-2	8.44485E-2
MLCM [30]	0.0	7.40512E-6	2.68680E-5	2.09157E-3	1.76603E-4	3.64289E-4
MVIM [28]	0.0	7.40792E-3	2.71193E-2	7.77909E-2	2.23924E-1	7.25885E-1

**Table 9.** Assessment of absolute errors for  $I(t)$  of the LWCM with other conventional methods relative to RK4-method.

$t$	0.1	0.2	0.4	0.6	0.8	1.0
LWCM	0.0	6.67521E-10	1.49248E-9	2.48213E-9	3.65587E-9	5.04227E-9
LADM [27]	0.0	8.27884E-10	2.42395E-9	1.23041E-8	6.98912E-8	3.01802E-7
VIM [28]	0.0	7.55394E-10	7.77006E-9	2.06505E-7	2.22150E-6	1.57157E-5
MLCM [30]	0.0	8.23268E-10	1.85483E-9	3.10779E-9	4.60980E-9	6.39965E-9
MVIM [28]	0.0	8.22679E-07	1.81560E-6	2.63240E-6	1.69902E-6	6.01179E-6

**Table 10.** Assessment of absolute errors for  $V(t)$  of the LWCM with other conventional methods relative to RK4 method.

$t$	0.1	0.2	0.4	0.6	0.8	1.0
LWCM	0.0	8.66885E-7	1.07285E-7	9.95660E-7	8.21068E-7	6.34323E-7
LADM [27]	0.0	8.94351E-7	1.20500E-5	2.14112E-4	1.53102E-3	6.95344E-3
VIM [28]	0.0	8.94261E-7	1.20708E-5	2.14112E-4	1.53573E-3	6.98260E-3
MLCM [30]	0.0	1.00440E-6	1.24243E-6	2.14112E-4	9.50322E-7	7.34076E-7
MVIM [28]	0.0	9.38641E-4	1.72757E-4	4.59167E-3	1.91046E-2	7.34076E-7

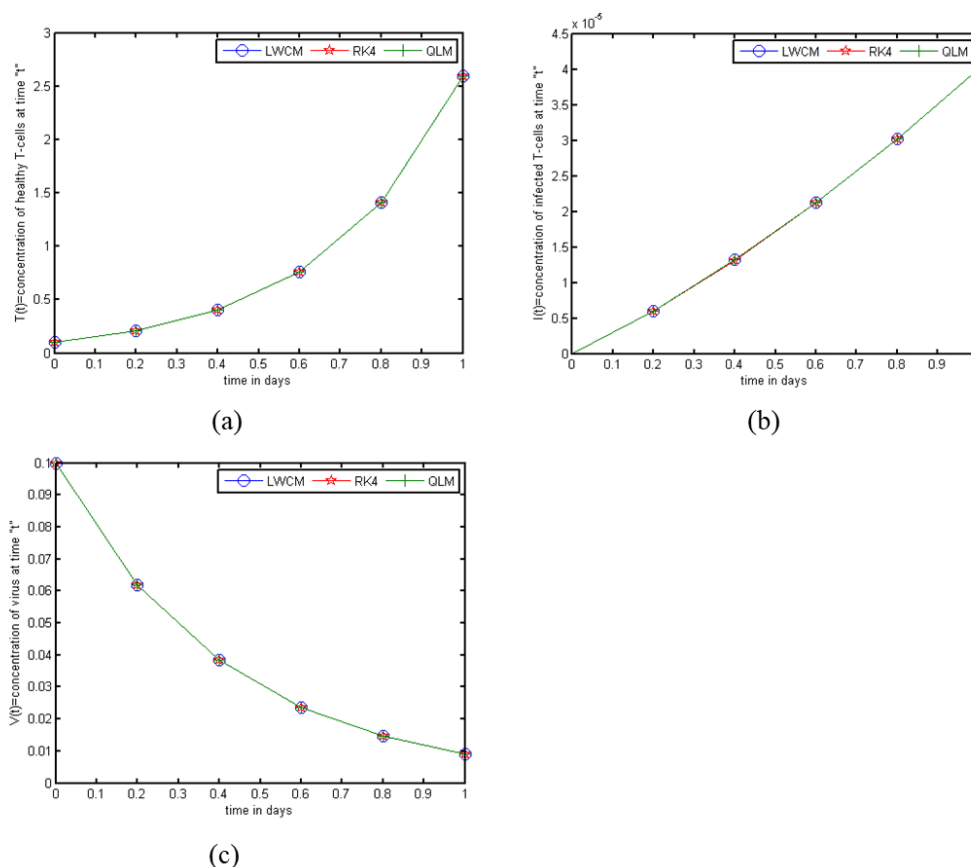


**Figure 1.** Graphical simulations for the findings of LWCM, RK4 and QLM schemes.

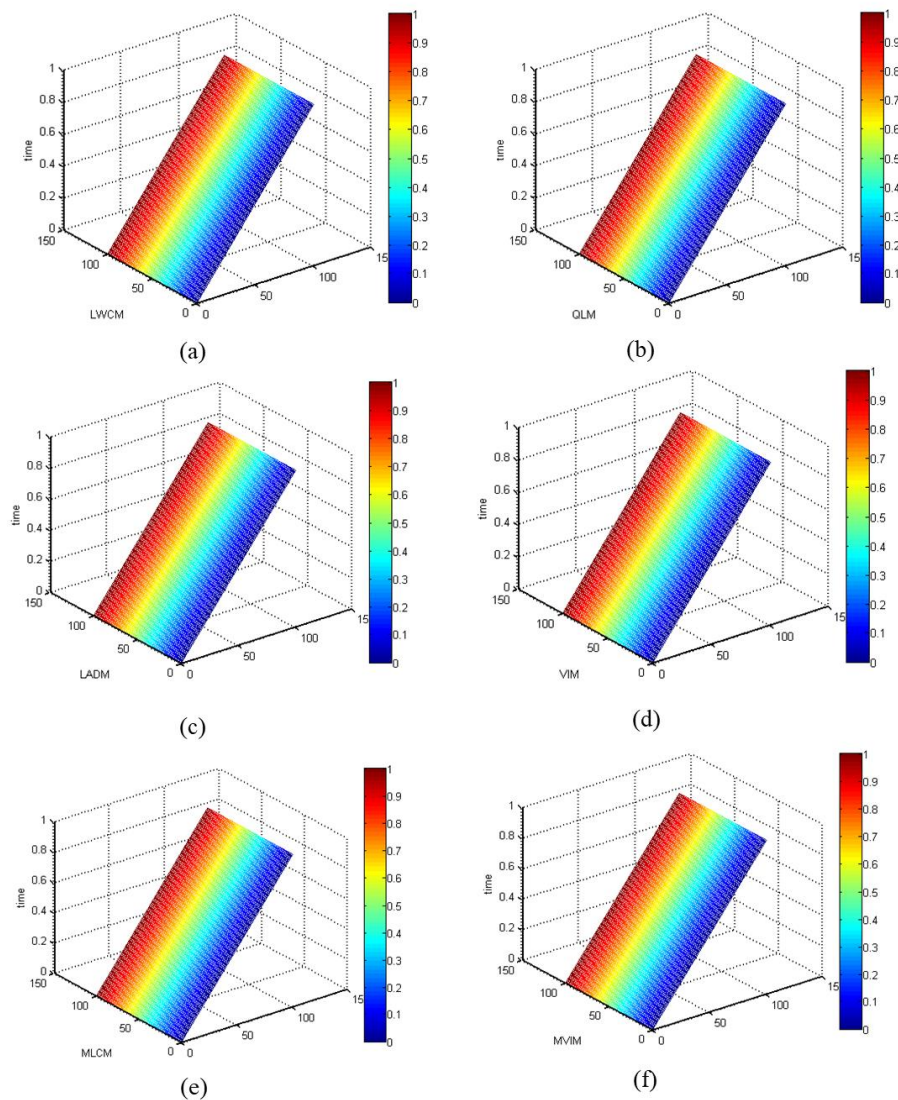


**Figure 2.** The mesh grid graphs of LAWCM, QLM, LADM, VIM, MLCM and MVIM schemes.

## 6. Modified formulation of the HIV infection model

The current antiretroviral combination of therapies is frequently used to treat HIV. As evidenced by the discovery of successful HIV medicines, understanding the fundamental causes of HIV infection has enabled the unprecedented development of novel therapies for the illness. Furthermore, because of major clinically controlled studies and an increasing understanding of the complexity of viral replication strategies for treating HIV infection were established concurrently. Treatments have an influence on the virus once it has entered into the cell. Chemotherapy, which is used to prevent the reproduction of HIV and changed the face of AIDS in the industrialized world. There has been a significant reduction in disease and mortality, as well as a decrease in healthcare consumption. HIV treatment has also revealed numerous new details on the pathogenesis, viral and cellular dynamics of HIV infection. However, the issues persist. Treatment does not stop HIV replication in all people, and the rise of drug-resistant viruses makes future treatment more difficult. Chronic treatment may

potentially cause toxicity. These challenges require the development of novel medications and treatment techniques to limit persistent viral replication. In this section, we developed a comprehensive mathematical model that characterized the dynamics of HIV infection by including a cure rate [47]. The cure rate contributes to a reduction in the infected cells and virus through enhancing human immunity and increases the concentration of healthy T-cells during the dynamical behavior after HIV infection. The novel model is described as follows:

$$\frac{dT}{dt} = \gamma - \omega T + \rho T \left(1 - \frac{T+I}{T_{max}}\right) - \chi VT + pI, \quad (6.1)$$

$$\frac{dI}{dt} = \chi VT - \delta I - pI, \quad (6.2)$$

$$\frac{dV}{dt} = N\delta I - dV. \quad (6.3)$$

In the above-mentioned model,  $T$  and  $I$  represent the concentration of healthy/infected cells, and  $V$  shows the population of virus particles. The initial conditions with an explanation of all the parameters involved in the model are presented in Table 1. The flow diagram of HIV infection is depicted in Figure 3. Following verification and reliability of the proposed LWCM method as well as code validation, we implemented the same method for the new model and graphically illustrated the solutions.

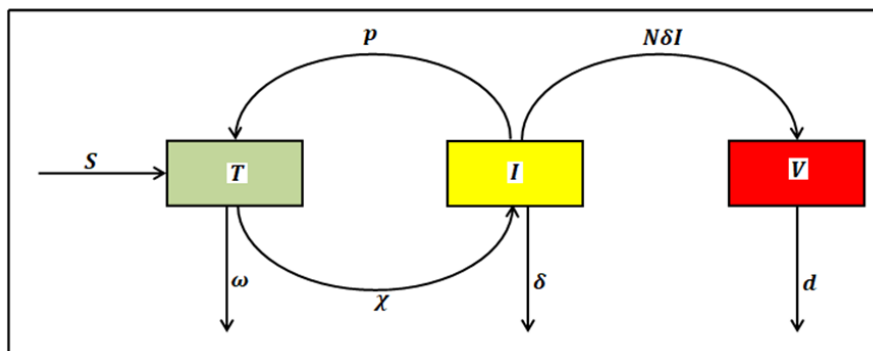


**Figure 3.** Flowchart of HIV transmission.

### 6.1. Basic reproduction number ( $R_0$ )

The most significant applications of basic reproduction number are determining whether an emerging infectious disease may spread in a community and predicting how many people need be inoculated by vaccination to eliminate a disease. Several variables influence the basic reproduction number, including the length of infectivity of afflicted persons, the infectiousness of the microorganism, and the number of susceptible people in the population that infected people encounter. The basic reproduction number  $R_0$  of an infection is the mean number of secondary cases caused by a single infected case in a fully susceptible individual. Mathematical analyses establish that the global dynamics of the spread of the HIV infectious disease are completely determined by the basic reproduction number. The infection will die out when  $R_0 < 1$ . If  $R_0 = 1$ , then the existing infection can cause disease that will stay alive and stable. If  $R_0 > 1$ , the infection has the potential to spread throughout a population. The larger the value of  $R_0$ , the more difficult it is to control the infection [48]. The value  $R_0$  of a disease is computed based on its infectious period, mode of transmission and

contact rate. A longer infectious period results in a higher value of  $R_0$ . The disease will be transmitted quickly, if an infected individual meets people who are not infected or vaccinated, therefore high contact rate results in high  $R_0$  value. The mode of transmission also contributes to the  $R_0$  value. We obtain the  $R_0$  for the given system using the Threshold theorem [49]. The Threshold theorem stated that if the epidemic will not get started unless the initial number of healthy cells exceeds a certain threshold values. i.e.,

if  $R_0 > 1$             epidemic  
 if  $R_0 > 1$             endemic  
 if  $R_0 = 1$             disease die out

## 6.2. Equilibria and local stability [35]

The nonnegative equilibria of system of Eqs (6.1)–(6.3) is  $E_0 = (T_0, 0, 0)$ ,  $\bar{E} = (\bar{T}, \bar{I}, \bar{V})$ , and we find  $T_0 = \frac{T_{\max}}{2\rho} \left( (\rho - \omega) \pm \sqrt{(\omega - \rho)^2 + 4\frac{\rho}{\gamma}} \right)$ .

For  $T_0$  we get positive and negative solutions. We are choosing the positive solution, which describes possible steady state of the system of Eqs (6.1)–(6.3) in the absence of virus particles.

$$\bar{T} = d \frac{(\delta + p)}{\chi N \delta}, \quad \bar{I} = \frac{1}{\delta} \left[ \gamma - \omega \bar{T} + \rho \bar{T} \left( 1 - \frac{\bar{T} + \bar{I}}{T_{\max}} \right) \right], \quad \bar{V} = \frac{R\delta}{d} \bar{I}.$$

The basic reproduction  $R_0 = \frac{T_0}{\bar{T}}$ . The significance of the value  $R_0$  is well known it is also known as the system's basic reproductive ratio. It depicts the average number of secondary infections caused by a single infected T-cell in a population of entirely susceptible T cells over the course of the infection. It helps to determine the dynamic characteristics of system of Eqs (6.1)–(6.3) over total time. We will now initiate to investigate the geometric features of system of Eqs (6.1)–(6.3) equilibria. Since  $T_0$  and  $\bar{T}$  satisfy

$$\begin{aligned} \gamma - \omega T_0 + \rho T_0 \left( 1 - \frac{T_0 + I_0}{T_{\max}} \right) &= 0, \\ \gamma - \omega \bar{T} + \rho \bar{T} \left( 1 - \frac{\bar{T} + \bar{I}}{T_{\max}} \right) &= \frac{1}{R\delta} [(N\delta \bar{T} - d(\delta + p))], \end{aligned}$$

we can get

$$\begin{aligned} \bar{T} > d \frac{(\delta + p)}{MN\delta} &\Rightarrow \gamma - \omega T_0 + \rho T_0 \left( 1 - \frac{T_0 + I_0}{T_{\max}} \right) > 0 \Rightarrow T_0 > \bar{T} \\ \bar{T} < d \frac{(\delta + p)}{\chi N \delta} &\Rightarrow \gamma - \omega T_0 + \rho T_0 \left( 1 - \frac{T_0 + I_0}{T_{\max}} \right) < 0 \Rightarrow T_0 < \bar{T}. \end{aligned}$$

Thus if  $R_0 > 1$ , then the positive equilibrium  $\bar{E} = (\bar{T}, \bar{I}, \bar{V})$  exists.

The Jacobean matrix of system of Eqs (6.1)–(6.3) is follows as

$$J = \begin{pmatrix} -\omega + \rho - \frac{2\rho T + \rho I}{T_{\max}} - MV & \frac{-\rho T}{T_{\max}} & -\chi T \\ \chi V & -(\delta + p) & \chi T \\ 0 & R\delta & -d \end{pmatrix}$$

Let  $E^* = (T^*, I^*, V^*)$  be any arbitrary equilibrium. Then the characteristic equation about  $E^*$  is given

by

$$\begin{vmatrix} \lambda + \omega - \rho + \frac{2\rho T^* + \rho I^*}{T_{\max}} + MV^* & \frac{\rho T^*}{T_{\max}} & \chi T^* \\ -\chi V & \lambda + \delta + p & -MT^* \\ 0 & -N\delta & \lambda + d \end{vmatrix} = 0. \quad (6.21)$$

For equilibrium  $E_0 = (T_0, 0, 0)$ , (6.21) reduces to

$$\left(\lambda + \omega - \rho + \frac{2\rho T_0}{T_{\max}}\right) [(\lambda^2 + \lambda(d + \delta + p) + d(\delta + p) - N\delta MT_0)] = 0. \quad (6.22)$$

Hence  $E_0 = (T_0, 0, 0)$  is locally asymptotically stable for  $R_0 < 1$ .

**Theorem 6.1.** (See [47]) If  $R_0 < 1$  then  $E_0 = (T_0, 0, 0)$  is locally asymptotically stable, if  $R_0 > 1$ ,  $E_0 = (T_0, 0, 0)$  is unstable.

**Theorem 6.2.** (See [47]) Let  $M > 0$  such that, for any positive solution  $(T(t), I(t), V(t))$  of system of Eqs (6.1)–(6.3),  $T(t) \leq M$ ,  $I(t) \leq M$  and  $V(t) \leq M$ , for all large  $t$ .

*Proof.* Let  $G_1(t) = T(t) + I(t)$ . Calculating the derivate of  $G_1(t)$  along the solution of system of Eqs (6.1)–(6.3), we find

$$\begin{aligned} \frac{dG_1(t)}{dt} &= \frac{dT}{dt} + \frac{dI}{dt} = \gamma - \omega T + \rho T \left(1 - \frac{T + I}{T_{\max}}\right) - \delta I \\ &= -\omega T - \delta I + \rho T - \frac{\rho T^2 + \rho TI}{T_{\max}} + \gamma \leq -hG_1(t) + M_0, \end{aligned}$$

where  $M_0 = \frac{T_{\max}\rho^2 + 4\rho\gamma}{4\rho}$ ,  $h = \min(\omega, \delta)$ . Then there exists  $M > 1$ , depending only the parameters of system of Eqs (6.1)–(6.3), such that  $G_1(t) < M$ , for all  $t$  large enough. Then  $T(t)$  and  $I(t)$  have the above bound. Its follow from the third equation of system of Eqs (6.1)–(6.3) that  $V(t)$  has an ultimately above bound, say, their maximum is  $M$ . The proof is complete.

Define  $D = \{(T, I, V) \in \mathbb{R}^3 : 0 < T \leq M, 0 < I \leq M, 0 < V \leq M\}$ . Obviously,  $D$  is convex.

**Theorem 6.3.** Suppose that

- 1)  $R_0 < 0$ ;
- 2)  $\left(d + \delta + p + \omega - \rho + \frac{2\rho\bar{T}\bar{I}}{T_{\max}} + \chi\bar{V}\right) \left[-\omega + \rho - \frac{2\rho\bar{T}\bar{I}}{T_{\max}}(d + \delta + p) + \chi\bar{V}(d + \delta)\right] > 0$ .

Then the positive equilibrium  $\bar{E} = (\bar{T}, \bar{I}, \bar{V})$ , Equations (6.21) reduces to

$$\lambda^3 + x_1\lambda^2 + x_2\lambda + x_3 = 0,$$

where

$$\begin{aligned} x_1 &= d + \delta + p + \omega - \rho + \frac{2\rho\bar{T}\bar{I}}{T_{\max}} + \chi\bar{V} > 0, \\ x_2 &= (\omega - \rho + \frac{2\rho\bar{T}\bar{I}}{T_{\max}})(d + \delta + p) - p\chi\bar{V} > 0, \\ x_3 &= d\delta\chi\bar{V} > 0. \end{aligned}$$

we also have

$$x_1x_2 - x_3 = \left(d + \delta + p + \omega - \rho + \frac{2\rho\bar{T}\bar{I}}{T_{\max}} + \chi\bar{V}\right) \left[\left(-\omega + \rho - \frac{2\rho\bar{T}\bar{I}}{T_{\max}}\right)(d + \delta + p) + \chi\bar{V}(d + \delta)\right] > 0.$$

By Routh-Hurwitz criterion [36], we have that  $\bar{E} = (\bar{T}, \bar{I}, \bar{V})$ , is locally asymptotically stable.

### 6.3. Global asymptotic stability

The global asymptotic stability of the illness steady state is discussed and describes the necessary conditions for a disease steady state that is globally asymptotically stable.

**Definition 6.1.** If any nonempty compact  $\omega$ -limit set of the system of Eqs (6.1)–(6.3) that contains no equilibria is a closed orbit, the system of Eqs (6.1)–(6.3) is said to satisfy the Poincare-Bendixson property [50].

**Definition 6.2.** (See [51]) The autonomous system of Eqs (6.1)–(6.3) is said to be competitive in  $D$  if, for some diagonal matrix  $Z = \text{diag}(\epsilon_1, \epsilon_2, \dots, \epsilon_n)$  where each  $\epsilon_i (i = 1, 2, \dots, n)$  is either 1 or  $-1$ ,  $Z \frac{\partial f}{\partial x} Z$  has no positive off diagonal elements for all  $x \in D$ .

**Theorem 3.4.** (See [51]) System of Eqs (6.1)–(6.3) is a competitive system.

*Proof.* By looking at the Jacobean matrix of system of the Eqs (6.1)–(6.3) and choosing the matrix  $Z$  as

$$Z = \begin{pmatrix} 1 & 0 & 0 \\ 0 & -1 & 0 \\ 0 & 0 & 1 \end{pmatrix}$$

In  $D$ , we see that the system of Eqs (6.1)–(6.3) is competitive, w.r.t the partial order defined by the orthant  $J = \{(T, I, V) \in \mathbb{R}^3 : T \leq 0, I \leq 0, V \leq 0\}$ . In fact, by simple calculating, we obtain

$$Z \frac{\partial f}{\partial x} Z = \begin{pmatrix} -\omega + \rho - \frac{2\rho T + \rho I}{T_{\max}} - MV & \frac{-\rho T}{T_{\max}} & -\chi T \\ \chi V & -\delta - p & -\chi T \\ 0 & -N\delta & -d \end{pmatrix}$$

**Remarks 6.1.** (See [52]) Since the system of Eqs (6.1)–(6.3) is competitive in  $D$  and  $D$  is convex. Then system of Eqs (6.1)–(6.3) satisfies the Poincare-Bendixson property.

**Lemma 6.1.** (See [52]) Assume that  $n = 3$  and  $D$  is convex. Suppose the system of Eqs (6.1)–(6.3) is competitive in  $D$  is convex. Suppose system of Eqs (6.1)–(6.3) is competitive in  $D$  and  $L$  is a nonempty compact omega limit set of system of Eqs (6.1)–(6.3). If  $L$  contains no equilibria, then  $L$  is a closed orbit.

The system of Eqs (6.1)–(6.3) has nontrivial periodic orbits, as shown by Remarks 3.3 and Lemma 3.3. Let  $A$  signify a linear operator on  $\mathbb{R}^n$ , as well as its matrix representation in terms of  $\mathbb{R}^n$ 's standard basis. Let  $\Lambda^2 \mathbb{R}^n$  denote the exterior product of  $\mathbb{R}^n$ . A matrix  $A$  induces canonically a linear operator  $A^{[2]}$  on  $\Lambda^2 \mathbb{R}^n$   $u_1, u_2 \in \mathbb{R}^n$ .

Define

$$A^{[2]}(u_1 \wedge u_2) = A(u_1) \wedge u_2 + A(u_2) \wedge u_1,$$

and extend the definition over  $\Lambda^2 \mathbb{R}^n$  by linearity. The second additive compound matrix of  $A$  is the matrix representation of  $A^{[2]}$  with respect to the canonically basis in  $\Lambda^2 \mathbb{R}^n$ . This is an  $\binom{n}{2} \times \binom{n}{2}$  matrix and satisfies the property  $(A + B)^{[2]} = A^{[2]} + B^{[2]}$ . In the special case when  $n = 2$ , we have  $A^{[2]}_{2 \times 2} = \text{tr } A$ . In general, each entry of  $A^{[2]}$  is a linear expression of those of  $A$ . For instance, when  $n = 3$ , the second additive compound matrix of  $A = (a_{ij})$  is

$$A^{[2]} = \begin{pmatrix} a_{11} + a_{22} & a_{23} & -a_{13} \\ a_{32} & a_{11} + a_{33} & a_{12} \\ -a_{31} & a_{21} & a_{22} + a_{33} \end{pmatrix}$$

The spectrum of  $A$  is  $\sigma A = \{\lambda_1, \dots, \lambda_n\}$ . Then  $\sigma A^{[2]} = \{\lambda_i + \lambda_j \mid 1 \leq i \leq j \leq n\}$  is spectrum of  $A^{[2]}$ .

Let  $x \mapsto f(x) \in \mathbb{R}^2$  be a  $C^1$  function for  $x$  in an open set  $D \in \mathbb{R}^n$ . Consider the differential equation  $\dot{x} = f(x)$ .

Let  $x(t, x_0)$  be the solution to the system of Eqs (6.1)–(6.3) such that  $x(t, x_0) = x_0$ . A set  $K$  is said to be absorbing in  $D$  for the system of Eqs (6.1)–(6.3), if  $x(t, K_1) \subset K$  for each compact  $K_1 \subset D$  and  $t$  sufficiently large. We make the following two basic assumptions:

(H<sub>1</sub>) There exists a compact absorbing set  $K \subset D$ .

(H<sub>2</sub>) System of Eqs (6.1)–(6.3) has a unique equilibrium  $\bar{x}$  in  $D$ .

If the equilibrium  $\bar{x}$  is locally stable and all trajectories in  $D$  converge to  $\bar{x}$ , it is said to be globally stable in  $D$ . If  $\bar{x}$  is globally stable in  $D$ , the assumptions (H<sub>1</sub>) and (H<sub>2</sub>) are satisfied. For virus models and many other biological models with a bounded cone as the feasible region, (H<sub>1</sub>) is equivalent to the uniform persistence of Eqs (6.1)–(6.3).

**Lemma 6.2.** (See [52]). A periodic orbit  $\Omega = \{\Phi(t); 0 < t < y\}$  of system of Eqs (6.1)–(6.3) is orbitally asymptotically stable with asymptotic phase if the linear system

$$Y'(t) = \frac{\partial f^{[2]}}{\partial x} \Phi(t)Y, \quad (2.3)$$

is asymptotically stable, where  $\frac{\partial f^{[2]}}{\partial x}$  is the second additive compound matrix of the Jacobian matrix  $\frac{\partial f^{[2]}}{\partial x}$  of  $f$ .

**Lemma 6.3.** (See [52]) Assume that

- 1) Assumptions that (H<sub>1</sub>) and (H<sub>2</sub>) hold.
- 2) Equations (6.1)–(6.3) satisfies the Poincare- Bendixson property.
- 3) For each periodic solution  $x = \Phi(t)$  with  $\Phi(0) \in D$ , the system of Eqs (6.1)–(6.3) is asymptotically stable.
- 4)  $\left( (-1)^n \det \left( \frac{\partial f}{\partial x}(\bar{x}) \right) \right) > 0$ .

Then the global asymptotically stable unique equilibrium  $\bar{x}$  exists in  $D$ .

#### 6.4. Results and discussions

Infection with the human immunodeficiency virus impairs the immune system, raises the risk of certain diseases, damages bodily organs such as the brain, kidneys, and heart, and causes mortality. Unfortunately, there is no treatment for this viral disorder at the moment. Although, there are effective retroviral medications for improving patients' health problems, excessive use of these treatments is not without risk. Therefore, we enhanced a mathematical model suggested by Parand et al. [32] by introducing the cure rate. The findings of the modified model with a cure rate are presented in this section. Our intention is to maximize the concentration of uninfected CD4+T cells in the body by using minimum drug therapies. We presented the findings of the new and old models in Figures 4(a)–(c). The novel model for the transmission dynamics of healthy T-cells, infected T-cells, and free HIV particles with a high cure rate produces more accurate results. This contributes to a decrease in infected

cells and viruses by improving human immunity. As immune cells diminish with the passage of time, the population of free viruses increases. Consequently, the number of free viruses and infected T-cells grows while the number of healthy T-cells decreases. The viruses infect healthy T-cells by attacking immune cells and transforming them into infected T-cells. The human body has the capacity to identify and fight these infections. T-cells are responsible for fighting against HIV viruses and for detecting and combating them. Figures 2(a)–(f) illustrate that an increase in T-cell potential results in an increase in the immune response and proliferation rate of healthy T-cells. Owing to this, the population of T-cells falls over time and reaches its lowest level, while the immunity level grows due to the generation of healthy T-cells, which kills the infected T-cells. Because of the decrease in infected T-cells, the number of T-cells rises once again and begins to fluctuate. If the long-term alterations in the T-cell response are insignificant, then the response cannot account for the decline in viral burden. From a biological point of view, it seems that activating T-cells makes it more likely that HIV infection will go away. Medically, it will provide physicians with enough information to lower the viral load of the illness. The model presented here is essential in the area of mathematical modeling of HIV infection of  $CD4^+$  T-cells. This will be utilized to evaluate the population dynamics of  $CD4^+$  T-cells in the presence and absence of HIV, which will be useful in observing clinical AIDS manifestations and suppressing the disease. The phase and chaotic behavior of the novel model are visualized in Figure 4(d) and Figure 5. Many scientific and engineering applications are based on a system's chaotic nature [53]. The chaotic diagrams demonstrate the feasibility and application of the suggested numerical approach, which may be generalized to novel chaotic systems. Although each phase diagram has a precisely distinct significance at each point, the accent is not on the extensive clinical interpretation of figures associated to solutions.

## 7. Conclusions

This research explained the computational and mathematical analysis of HIV models. We used an innovative numerical scheme called the Legendre wavelet collocation scheme and contrasted the absolute errors between the current solutions and existing findings relative to the well-known Runge-Kutta scheme. In comparison to the outcomes of other schemes, the LWCM results were found to be more accurate and reliable. Relying on these assertions, the new scheme is a superior approach for time-dependent problems, with better approximate solutions. On the other hand, we introduced a novel HIV/AIDS epidemic model with a cure rate and assessed the stability of the model based on the reproduction number. The basic reproduction number determines the global dynamics of our model. It could be seen that the disease-free equilibrium is globally asymptotically stable when it is less than unity and unstable when it becomes greater than unity. The mathematical analysis of the proposed model, validated by the numerical simulation results, shows the effectiveness of the model in maximizing the concentration of uninfected  $CD4^+$  T cells, minimizing the concentrations of infected cells and free virions in the body with a minimum dose of a combination of drug therapies in order to avoid the adverse effects associated with excessive use of drugs. It could be observed that the treatment rate produces more accurate and strengthens the human immune system, which contributes to a reduction in infected cells and viruses. From the study, medical physicians can become knowledgeable about the dynamical behavior of healthy and infected T cells and viruses during disease.

Besides, it is a worthwhile area of study to investigate whether or not the approaches used in this manuscript are beneficial to other epidemic models, such as the rabies transmission model, the malaria

transmission model, and the syphilis transmission model.

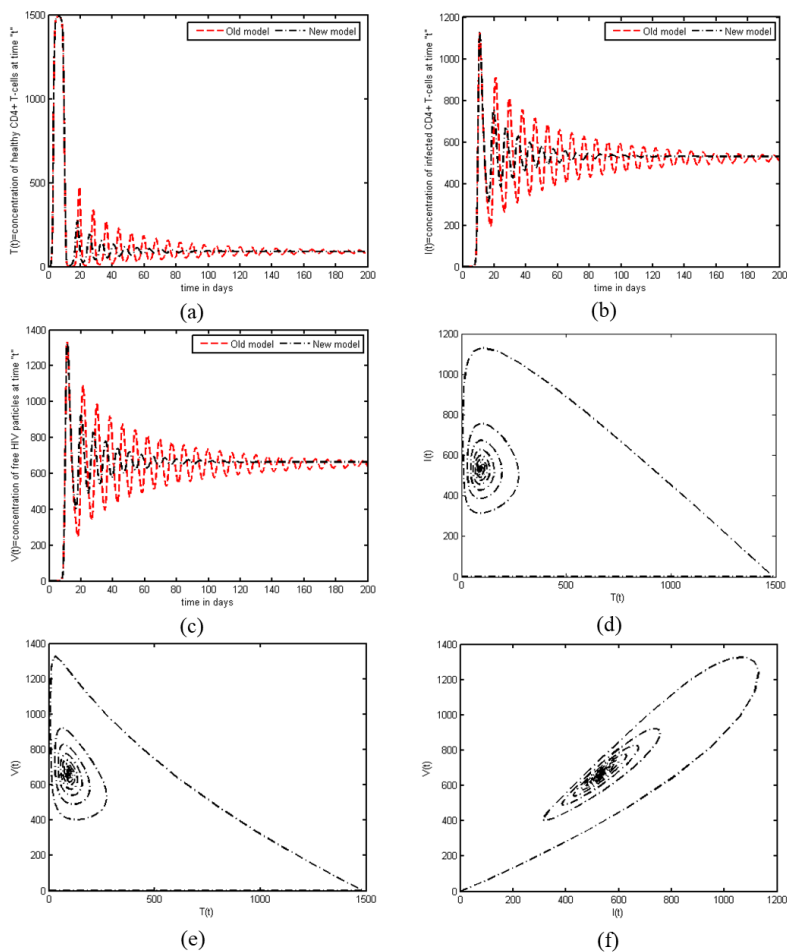


**Figure 4.** The geometrical comparison of new and old HIV models and a phase portrait diagram of the new model.

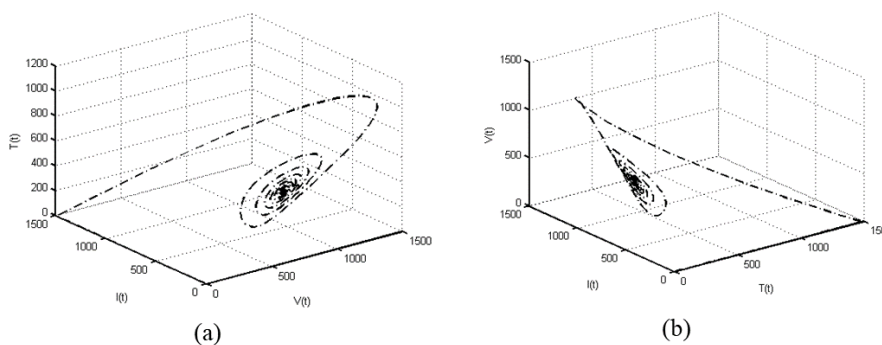


**Figure 5.** The phase diagram for the state variables of the new model.

## Acknowledgments

The authors would like to thank the reviewers and the editor for their valuable and fruitful comments and appreciated their suggestions to improve the quality of manuscript. The author Attaullah would like to thank Mr. Muhammad Shakeel Khan department of mathematics & Statistics and Mr. Sami Ullah department of Economics for their support and suggestions.

## Conflict of interest

The authors declare that they have no known competing financial interests or personal relationships that could have appeared to influence the work reported in this paper.

## References

1. J. M. Hyman, J. Li, E. A. Stanley, The differential infectivity and staged progression models for the transmission of HIV, *Math. Biosci.*, **155** (1999), 77–109. [https://doi.org/10.1016/S0025-5564\(98\)10057-3](https://doi.org/10.1016/S0025-5564(98)10057-3)
2. X. D. Lin, H. W. Hethcote, P. Van den Driessche, An epidemiological model for HIV/AIDS with proportional recruitment, *Math. Biosci.*, **118** (1993), 181–195. [https://doi.org/10.1016/0025-5564\(93\)90051-B](https://doi.org/10.1016/0025-5564(93)90051-B)
3. C. C. McCluskey, A model of HIV/AIDS with staged progression and amelioration, *Math. Biosci.*, **181** (2003), 1–16. [https://doi.org/10.1016/S0025-5564\(02\)00149-9](https://doi.org/10.1016/S0025-5564(02)00149-9)
4. T. Bastys, V. Gapsys, N. T. Doncheva, R. Kaiser, B. L. de Groot, O. V. Kalinina, Consistent prediction of mutation effect on drug binding in HIV-1 protease using alchemical calculations, *J. Chem. Theory Comput.*, **14** (2018), 3397–3408. <https://doi.org/10.1021/acs.jctc.7b01109>
5. H. B. Guo, Y. L. Michael, Global dynamics of a staged-progression model for HIV/AIDS with amelioration, *Nonlinear Anal.-Real*, **12** (2011), 2529–2540. <https://doi.org/10.1016/j.nonrwa.2011.02.021>
6. M. E. Schechter, B. B. Andrade, T. Y. He, G. H. Richter, K.W. Tosh, B. B. Policicchio, et al., Inflammatory monocytes expressing tissue factor drive SIV and HIV-coagulopathy, *Sci. Transl. Med.*, **9** (2017), eaam5441. <https://doi.org/10.1126/scitranslmed.aam5441>
7. A. Yusuf, U. T. Mustapha, T. A. Sulaiman, E. Hincal, M. Bayram, Modeling the effect of horizontal and vertical transmissions of HIV infection with Caputo fractional derivative, *Chaos Soliton. Fract.*, **145** (2021), 110794. <https://doi.org/10.1016/j.chaos.2021.110794>
8. H. Singh, Analysis of drug treatment of the fractional HIV infection model of CD4<sup>+</sup> T-cells, *Chaos Soliton. Fract.*, **146** (2021), 110868. <https://doi.org/10.1016/j.chaos.2021.110868>
9. S. Thirumalai, R. Seshadri, S. Yuzbasi, Spectral solutions of fractional differential equations modeling combined drug therapy for HIV infection, *Chaos Soliton. Fract.*, **151** (2021), 111234. <https://doi.org/10.1016/j.chaos.2021.111234>
10. N. H. Al Shamrani, Stability of a general adaptive immunity HIV infection model with silent infected cell-to-cell spread, *Chaos Soliton. Fract.*, **150** (2021), 110422. <https://doi.org/10.1016/j.chaos.2020.110422>
11. Fatmawati, M.A. Khan, H. P. Odinsyah, Fractional model of HIV transmission with awareness effect, *Chaos Soliton. Fract.*, **138** (2020), 109967. <https://doi.org/10.1016/j.chaos.2020.109967>

12. A. H. Abdel-Aty, M. M. A. Khater, H. Dutta, J. Bouslimi, M. Omri, Computational solutions of the HIV-1 infection of CD4<sup>+</sup> T-cells fractional mathematical model that causes acquired immunodeficiency syndrome (AIDS) with the effect of antiviral drug therapy, *Chaos Soliton. Fract.*, **139** (2020), 110092. <https://doi.org/10.1016/j.chaos.2020.110092>
13. A. Singh, B. Razooky, C. D. Cox, M. L. Simpson, L. S. Weinberger, Transcriptional bursting from the HIV-1 promoter is a significant source of stochastic noise in HIV-1 gene expression, *Biophys. J.*, **98** (2010), L32–L34. <https://doi.org/10.1016/j.bpj.2010.03.001>
14. X. R. Mao, G. Marion, E. Renshaw, Environmental Brownian noise suppresses explosions in population dynamics, *Stoch. Proc. Appl.*, **97** (2002), 95–110. [https://doi.org/10.1016/S0304-4149\(01\)00126-0](https://doi.org/10.1016/S0304-4149(01)00126-0)
15. O. M. Ogunlaran, S. C. O. Noutchie, Mathematical model for an effective management of HIV infection, *BioMed Res. Int.*, **2016** (2016), 4217548. <https://doi.org/10.1155/2016/4217548>
16. R. P. Duffin, R. H. Tullis, Mathematical models of the complete course of HIV infection and AIDS, *Comput. Math. Method. M.*, **4** (2002), 826239. <https://doi.org/10.1080/1027366021000051772>
17. E. O. Omondi, R. W. Mbogo, L. S. Luboobi, Mathematical modelling of the impact of testing, treatment and control of HIV transmission in Kenya, *Cogent Math. Stat.*, **5** (2018), 1475590. <https://doi.org/10.1080/25742558.2018.1475590>
18. D. Wodarz, M. A. Nowak, Mathematical models of HIV pathogenesis and treatment, *Bio. Essays*, **24** (2002), 1178–1187. <https://doi.org/10.1002/bies.10196>
19. A. Ida, S. Oharu, Y. Oharu, A mathematical approach to HIV infection dynamics, *J. Comput. Appl. Math.*, **204** (2007), 172–186. <https://doi.org/10.1016/j.cam.2006.04.057>
20. A. Mastroberardino, Y. J. Cheng, A. Abdelrazec, H. Liu, Mathematical modeling of the HIV/AIDS epidemic in Cuba, *Int. J. Biomath.*, **8** (2015), 1550047. <https://doi.org/10.1142/S1793524515500473>
21. Attaullah, M. Sohaib, Mathematical modeling and numerical simulation of HIV infection model, *Res. Appl. Math.*, **7** (2020), 100118. <https://doi.org/10.1016/j.rinam.2020.100118>
22. K. Theys, P. Libin, A. C. Pineda-Pena, A. Nowe, A. M. Vandamme, A. B. Abecasis, The impact of HIV-1 within-host evolution on transmission dynamics, *Curr. Opin. Virol.*, **28** (2018), 92–101. <https://doi.org/10.1016/j.coviro.2017.12.001>
23. F. Bozkurt, F. Peker, Mathematical modelling of HIV epidemic and stability analysis, *Adv. Differ. Equ.*, **2014** (2014), 95. <https://doi.org/10.1186/1687-1847-2014-95>
24. E. A. Nosova, A. A. Romanyukha, Mathematical model of HIV-infection transmission and dynamics in the size of risk groups, *Math. Models Comput. Simul.*, **5** (2013), 379–393. <https://doi.org/10.1134/S207004821304011X>
25. X. D. Sun, H. Nishiura, Y. N. Xiao, Modeling methods for estimating HIV incidence: A mathematical review, *Theor. Biol. Med. Model.*, **17** (2020), 1. <https://doi.org/10.1186/s12976-019-0118-0>
26. N. H. Sweilam, S. M. AL-Mekhlafi, Z. N. Mohammed, D. Baleanu, Optimal control for variable order fractional HIV/AIDS and malaria mathematical models with multi-time delay, *Alex. Eng. J.*, **59** (2020), 3149–3162. <https://doi.org/10.1016/j.aej.2020.07.021>
27. M. Y. Ongun, The Laplace Adomian decomposition method for solving a model for HIV infection of CD4<sup>+</sup> T cells, *Math. Comput. Model.*, **53** (2011), 597–603. <https://doi.org/10.1016/j.mcm.2010.09.009>

28. M. Merdan, A. Gokdogan, A. Yildirim, On the numerical solution of the model for HIV infection of  $CD4^+$  T cells *Comput. Math. Appl.*, **62** (2011) 118–123. <https://doi.org/10.1016/j.camwa.2011.04.058>
29. Ş. Yüzbaşı, A numerical approach to solve the model for HIV infection of  $CD4^+$  T cells, *Appl. Math. Model.*, **36** (2012), 5876–5890. <https://doi.org/10.1016/j.apm.2011.12.021>
30. N. Doğan, Numerical treatment of the model for HIV infection of  $CD4^+$  T cells by using multistep Laplace Adomian decomposition method, *Discrete Dyn. Nat. Soci.*, **2012** (2012), 976352. <https://doi.org/10.1155/2012/976352>
31. M.R. Gandomani, M. T. Kajani, Numerical solution of a fractional order model of HIV infection of  $CD4^+$  T cells using Müntz-Legendre polynomials, *Inte. J. Bioautomation*, **20** (2016), 193–204.
32. K. Parand, Z. Kalantari, M. Delkhosh, Quasilinearization-Lagrangian method to solve the HIV infection model of  $CD4^+$  T-cells, *SeMA J.*, **75** (2018), 271–283. <https://doi.org/10.1007/s40324-017-0133-1>
33. Attaullah, R. Drissi, W. Weera, Galerkin time discretization scheme for the transmission dynamics of HIV infection with non-linear supply rate, *AIMS Mathematics*, **7** (2022), 11292–11310. <https://doi.org/10.3934/math.2022630>
34. Z. Iqbal, N. Ahmed, D. Baleanu, W. Adel, M. Rafiq, M. A. ur Rehman, et al., Positivity and boundedness preserving numerical algorithm for the solution of fractional nonlinear epidemic model of HIV/AIDS transmission, *Chaos Soliton. Fract.*, **134** (2020), 109706. <https://doi.org/10.1016/j.chaos.2020.109706>
35. H. Günerhan, H. Dutta, M. A. Dokuyucu, W. Adel, Analysis of a fractional HIV model with Caputo and constant proportional Caputo operators, *Chaos Soliton. Fract.*, **139** (2020), 110053. <https://doi.org/10.1016/j.chaos.2020.110053>
36. W. Gao, H. Günerhan, H. Me. Baskonus, Analytical and approximate solutions of an epidemic system of HIV/AIDS transmission, *Alex. Eng. J.*, **59** (2020), 3197–3211. <https://doi.org/10.1016/j.aej.2020.07.043>
37. M. Sohaib, S. Haq, S. Mukhtar, I. Khan, Numerical solution of sixth-order boundary-value problems using Legendre wavelet collocation method, *Res. Phys.*, **8** (2018), 1204–1208. <https://doi.org/10.1016/j.rinp.2018.01.065>
38. S. ul Islam, I. Aziz, A. S. Al-Fhaid, A. Shah, A numerical assessment of parabolic partial differential equations using Haar and Legendre wavelets, *Appl. Math. Model.*, **37** (2013), 9455–9481. <https://doi.org/10.1016/j.apm.2013.04.014>
39. M. H. Heydari, M. R. Hooshmandasl, F. M. M. Ghaini, C. Cattani, Wavelets method for the time fractional diffusion-wave equation, *Phys. Lett. A*, **379** (2015), 71–76. <https://doi.org/10.1016/j.physleta.2014.11.012>
40. M. H. Heydari, M. R. Hooshmandasl, F. M. M. Ghaini, F. Fereidouni, Two-dimensional Legendre wavelets for solving fractional Poisson equation with Dirichlet boundary conditions, *Eng. Anal. Bound. Elem.*, **37** (2013), 1331–1338. <https://doi.org/10.1016/j.enganabound.2013.07.002>
41. K. Dizicheh, F. Ismail, M. T. Kajani, M. Maleki, A Legendre wavelet spectral collocation method for solving oscillatory initial value problems, *J. Appl. Math.*, **2013** (2013), 591636. <https://doi.org/10.1155/2013/591636>
42. M. T. Kajani, A. H. Vencheh, Solving linear integro-differential equation with Legendre wavelets, *Int. J. Comput. Math.*, **81** (2004), 719–726. <https://doi.org/10.1080/00207160310001650044>

43. D. Abbaszadeh, M. T. Kajani, M. Momeni, M. Zahraei, M. Maleki, Solving fractional Fredholm integro–differential equations using Legendre wavelets, *Appl. Numer. Math.*, **166** (2021), 168–185. <https://doi.org/10.1016/j.apnum.2021.04.008>
44. M. Razzaghi, S. Yousefi, Legendre wavelets direct method for variational problems, *Math. Comput. Simul.*, **53** (2020), 185–192. [https://doi.org/10.1016/S0378-4754\(00\)00170-1](https://doi.org/10.1016/S0378-4754(00)00170-1)
45. M. Kutta, Beitrag zur naehrungsweisen integration totaler differential gleichungen, *Z. Math. Phys.*, **46** (1901), 435–453.
46. Attaullah, R. Jan, A. Jabeen, Solution of the HIV infection model with full logistic proliferation and variable source term using Galerkin scheme, *Matrix Sci. Math.*, **4** (2020), 37–43. <https://doi.org/10.26480/msmk.02.2020.37.43>
47. X. Y. Zhou, X. Y. Song, X. Y. Shi, A differential equation model of HIV infection of CD4<sup>+</sup> T-cells with cure rate, *J. Math. Anal. Appl.*, **342** (2008), 1342–1355. <https://doi.org/10.1016/j.jmaa.2008.01.008>
48. R. N. Nsubuga, R. G. White, B. N. Mayanja, L. A. Shafer, Estimation of the HIV basic reproduction number in rural south west Uganda: 1991–2008, *Plos One*, **9** (2014), e83778. <https://doi.org/10.1371/journal.pone.0083778>
49. Z. M. Chen, X. X. Liu, L. L. Zeng, Threshold dynamics and threshold analysis of HIV infection model with treatment, *Adv. Differ. Equ.*, **2020** (2020), 597. <https://doi.org/10.1186/s13662-020-03057-2>
50. J. W. Jia, G. L. Qin, Stability analysis of HIV/AIDS epidemic model with nonlinear incidence and treatment, *Adv. Differ. Equ.*, **2017** (2017), 136. <https://doi.org/10.1186/s13662-017-1175-5>
51. H. L. Smith, *Monotone dynamical systems: An introduction to the theory of competitive and cooperative systems*, American Mathematical Society, 1995. <https://doi.org/10.1090/surv/041>
52. M. Y. Li, L. C. Wang, Global stability in some SEIR epidemic models. In: *Mathematical approaches for emerging and reemerging infectious diseases: models, methods, and theory*, New York: Springer, 2002, 295–311. [https://doi.org/10.1007/978-1-4613-0065-6\\_17](https://doi.org/10.1007/978-1-4613-0065-6_17)
53. Attaullah, R. Jan, Ş. Yüzbaşı, Dynamical behaviour of HIV Infection with the influence of variable source term through Galerkin method, *Chaos Soliton. Fract.*, **152** (2021), 111429. <https://doi.org/10.1016/j.chaos.2021.111429>



AIMS Press

© 2022 the Author(s), licensee AIMS Press. This is an open access article distributed under the terms of the Creative Commons Attribution License (<http://creativecommons.org/licenses/by/4.0>)